

Research Article

Decomposition and Mineralization of Dimethyl Phthalate in an Aqueous Solution by Wet Oxidation

Dar-Ren Ji,¹ Chia-Chi Chang,¹ Shih-Yun Chen,¹ Chun-Yu Chiu,²
Jyi-Yeong Tseng,¹ Ching-Yuan Chang,^{1,3} Chiung-Fen Chang,⁴ Sheng-Wei Chiang,⁵
Zang-Sie Hung,¹ Je-Lueng Shie,⁶ Yi-Hung Chen,⁷ and Min-Hao Yuan^{1,7}

¹Graduate Institute of Environmental Engineering, National Taiwan University, Taipei 106, Taiwan

²Department of Cosmetic Science and Application, Lan Yang Institute of Technology, Yilan 261, Taiwan

³Department of Chemical Engineering, National Taiwan University, Taipei 106, Taiwan

⁴Department of Environmental Science and Engineering, Tunghai University, Taichung 407, Taiwan

⁵Chemical Engineering Division, Institute of Nuclear Energy Research, Atomic Energy Council, Lungtan, Taoyuan 325, Taiwan

⁶Department of Environmental Engineering, National Ilan University, Yilan 260, Taiwan

⁷Department of Chemical Engineering and Biotechnology, National Taipei University of Technology, Taipei 106, Taiwan

Correspondence should be addressed to Ching-Yuan Chang; cychang3@ntu.edu.tw

Received 10 November 2014; Revised 23 May 2015; Accepted 10 June 2015

Academic Editor: Zulin Zhang

Copyright © 2015 Dar-Ren Ji et al. This is an open access article distributed under the Creative Commons Attribution License, which permits unrestricted use, distribution, and reproduction in any medium, provided the original work is properly cited.

Dimethyl phthalate (DMP) was treated via wet oxygen oxidation process (WOP). The decomposition efficiency η_{DMP} of DMP and mineralization efficiency η_{TOC} of total organic carbons were measured to evaluate the effects of operation parameters on the performance of WOP. The results revealed that reaction temperature T is the most affecting factor, with a higher T offering higher η_{DMP} and η_{TOC} as expected. The η_{DMP} increases as rotating speed increases from 300 to 500 rpm with stirring enhancement of gas liquid mass transfer. However, it exhibits reduction effect at 700 rpm due to purging of dissolved oxygen by overstirring. Regarding the effects of pressure P_T , a higher P_T provides more oxygen for the forward reaction with DMP, while overhigh P_T increases the absorption of gaseous products such as CO_2 and decomposes short-chain hydrocarbon fragments back into the solution thus hindering the forward reaction. For the tested P_T of 2.41 to 3.45 MPa, the results indicated that 2.41 MPa is appropriate. A longer reaction time of course gives better performance. At 500 rpm, 483 K, 2.41 MPa, and 180 min, the η_{DMP} and η_{TOC} are 93 and 36%, respectively.

1. Introduction

Phthalic acid esters (PAEs) including dimethyl phthalate (DMP) are major plasticizer to improve the mechanical properties of polymers. These polymers in turn were used for making tableware such as forks, spoons, dishes, cups, and lunchboxes. In fact, the PAEs are added via noncovalent bonding with the polymers. It means PAEs are easily released to the hot soup, heated food, and oily contents from the tableware and are orally ingested daily [1, 2].

PAEs are endocrine disrupter substances (EDSs) too. Their derivatives exhibit the similar structure with endocrine of human and other animals, thus inducing the possibility of

cancer of human and the sex development of male. The worst influence of EDSs to the ecosystem would be extinction for endanger species [3, 4].

Although PAEs can be effectively removed from the aqueous phase by adsorption [5] which also has been applied to treat other EDSs [6, 7], it needs the regeneration of exhausted adsorbent and the post treatment of concentrated regeneration solution. Activated sludge based biological sewage treatment system needs 20 d to reach 71% mineralization efficiency and is not beneficial to deal with toxic DMP. It was biodegraded to monomethyl phthalate (MMP) and phthalic acid (PA) after treatment of 2.5 d [8–10]. Some advanced solutions were proposed such as photolysis [11–13], photocatalysis

[11–15], electrochemical [16, 17], and oxidant-added oxidation [11, 14, 18, 19] methods. Most of these treatments need postbiological process to further mineralize the decomposed compounds. The unconsumed oxidant residue needs to be neutralized for matching the effluent standard [14, 15]. Processes of wet air oxidation (WAP) and wet oxygen oxidation (WOP) with (CWAP and CWOP) and without catalysts have been successfully employed for oxidation treatments [20–30]. For example, in a study on the treatment of high-strength industrial wastewater, Lin and Ho [27] reported that the chemical oxygen demand (COD) removal efficiencies (η_{COD}) via WAP, WOP, and CWAP with CuSO_4 catalyst were 65, 73, and 75%, respectively, at 473 K, 3 MPa, 300 rpm, 1 L/min gas flow rate, and 2 h. The application of WAP and WOP has the advantages avoiding the posttreatment of unwanted residual oxidant species and no need for the recovery and regeneration of catalyst, compared with oxidant-added oxidation and catalytic oxidation, respectively. The abundant dissolved oxygen left can improve the performance of regular biological sewage system if needed [18]. Moreover, WOP gives η_{COD} only slightly less than catalytic oxidation while higher than WAP. This study thus employed WOP to treat the DMP-containing aqueous solution.

2. Experimental Materials and Methods

2.1. Materials. DMP with purity of 99.5% was supplied by Hayashi Pure Chemical Industries Ltd. (Osaka, Japan). The mobile phase of high performance liquid chromatography (HPLC) was composed as acetonitrile (CH_3CN) : DI water = 1 : 1, where acetonitrile of 100% purity was from J. T. Baker, Phillipsburg, NJ. The solvent for apparatus cleaning is acetone ($\text{C}_3\text{H}_4\text{O}$) with purity of 99.5% by Mallinckrodt Chemicals, St. Louis, MD. The reagents for measurement of total organic carbon (TOC) were (1) carrier gas: 99.99% N_2 from San Fu Chemical Co. Ltd., Taipei, Taiwan; (2) oxidant: sodium peroxydisulfate, $\text{Na}_2\text{S}_2\text{O}_8$ (99% purity), from Nacalai Tesque, Kyoto, Japan; (3) standard solution: anhydrous potassium biphthalate, KHP, $\text{C}_8\text{H}_5\text{KO}_4$ (99.0% purity), from Riedel-de Haën, Seelze, Germany. The reaction gas O_2 (99.99% purity) and air (O_2 : N_2 = 20 : 80, 99.99% purity) were purchased from San Fu Chemical Co. Ltd., Taipei, Taiwan.

2.2. Methods. The pressurized autoclave reaction system is shown in Figure 1. A 1 L bench top reactor is used. It is made of stainless steel 316 and equipped with a stirring rotor (DC-2RT44, Hsing-Tai Machinery Ind. Co., Taipei, Taiwan), pressure display module, and K-type thermal couple. The temperature of heater (Model-TC-10A, Macro Fortunate, Taipei, Taiwan) is controlled with temperature controller (Model-BMW-500, Newlab Instrument Co., Taipei, Taiwan). Mass flow controller of Model 5850E manufactured by Brooks (Hatfield, PA) is employed to control the gas flow rate. The bearing is cooled by cooling water from circulating bath (Model-B403, Firstek Scientific, Taipei, Taiwan). The upper cap of vessel has six holes with five for two sampling valves, thermal couple, pressure gauge, and release valve, while one for spare port. The experiments were batch type with volume

TABLE 1: Operation parameters and range of WOP.

Parameter of operation	Operation range
Rotation speed Nr, rpm	300, 500, 700
Temperature T , K	463, 473, 483
Pressure P_T , MPa	2.41, 2.67, 3.10, 3.45
Working gas of O_2	Pure O_2

of liquid of DMP solution (V_L) of 400 mL. The sampling valves are connected to cooling coil. The pressured vapor was captured to the coil and then cooled while keeping the pressure of the reactor. After 5 mL liquor was sampled, the noncollected cooled liquid was conducted back to the reactor.

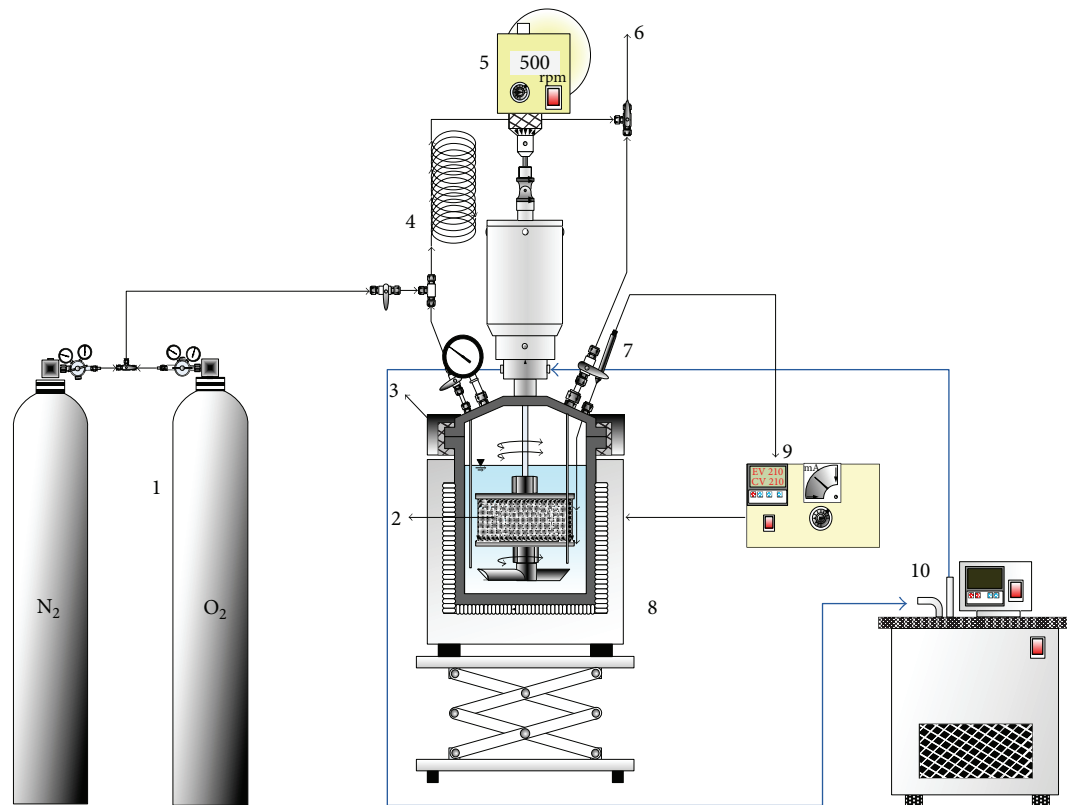
The initial concentration (C_0) of DMP solution was 100 mg/L. The concentrations of DMP of samples (C) were analyzed by high performance liquid chromatography (HPLC, Viscotek Model 500, Houston, TX), while those of total organic carbon (TOC) were analyzed by TOC analyzer (Model 1010, O.I. Analytical, NY). The column of HPLC is 516C-18 of 25 cm \times 4.6 mm with ID 5 μm (Supelco Inc., Bellefonte, PA). The TOC analyzer uses nondispersive infrared (NDIR) detector, with carrier gas of N_2 , oxidative agent of 10% sodium peroxydisulfate solution, and TOC standard solution of anhydrous potassium biphthalate. The precision of experimental data was indicated in figures by error bar with standard deviation (σ_{n-1}) above and below the average value.

The batch WOP process was performed in two stages. The first is heating stage. The DMP-containing solution, which was prebubbled by N_2 to purge out the residual oxygen, was filled into the autoclave reactor and then heated from room temperature 283 K to the set reaction temperature (T) without any oxidant. The tested temperatures were 463, 473, and 483 K. The initial time (t) was noted as 0_i , while the final time of the first stage as 0_f . In the second stage, the working gas O_2 was introduced into the reactor at $t = 0_f$ to the desired operation pressure (P_T) to continue the oxygen oxidation reaction.

The major operation parameters of batch WOP were examined including (1) the stirring speed (Nr), (2) reaction temperature T , and (3) operation pressure P_T . The initial pH value (pH_0) was not adjusted while reflected by the C_0 . Values of parameters are listed in Table 1 referring to those of others [27, 29]. For example, Lin and Ho [27] performed the experiments with Nr = 100–400 rpm, P_T = 2.5–5.0 MPa, and T = 423–513 K. They reported that (1) 300 rpm and 3 MPa were appropriate and (2) T was the most important operation variable with marginal enhancing effect for T above 498 K. The present study extended Nr to 500–700 rpm, while it employed P_T and T in the proper ranges of those of Lin and Ho [27].

3. Results and Discussion

3.1. Effects of Rotation Speeds Nr. Figure 2 illustrate the variation of decomposition efficiency of DMP (η_{DMP}) with reaction time t at various rotation speeds (Nr = 300, 500,



- | | | |
|------------------|-------------------|----------------------------|
| (1) Gas cylinder | (5) Rotor | (9) Temperature controller |
| (2) Net | (6) Sampling port | (10) Circulating bath |
| (3) Reactor | (7) Thermal probe | |
| (4) Cooling loop | (8) Heater | |

FIGURE 1: Schematic diagram of wet oxygen oxidation system.

and 700 rpm). Other conditions are reaction temperature $T = 473$ K and operation pressure $P_T = 2.41$ MPa. As expected, more DMP is decomposed with longer t giving higher η_{DMP} . The η_{DMP} is 66, 78, and 66% at $t = 180$ min for $Nr = 300$, 500, and 700 rpm, respectively. In general, a good gas liquid mixing assists the reaction. Thus, an increase of Nr from 300 to 500 rpm increases the gas liquid mass transfer and offers a higher η_{DMP} . However, the dissolved oxygen needed for reaction may be tripped or purged out from liquid to gas as further increasing the Nr , say to 700 rpm, reducing the η_{DMP} . The Nr of 500 rpm leads to better increasing trend of η_{DMP} .

It is noted that although the effects of Nr of low rpm, say below 300 rpm, on the system performance were not investigated in this study, its qualitative effects may be realized referring to the work of Lin and Ho [27] dealing with the treatment of high-strength industrial wastewater. They examined the effects of Nr from 100 to 400 rpm on the chemical oxygen demand removal efficiencies η_{COD} , indicating apparently significant effect as Nr below 300 rpm. An Nr of 300 rpm

was thus adopted for their further experiments. This thus justified the adoption of 500 rpm for the followed experiments of the present study, assuring the good mixing.

The effect of reaction time on the pH value of DMP-containing solution during WOP at different Nr is depicted in Figure 3. The decrease of pH value as oxidation decomposition takes place indicates the formation of acidic products. Although the decompositions are significant from 60 to 180 min as shown in Figure 2, the pH value stays nearly the same at about 4 after 60 min. This might be due to the cause that some intermediate acidic products from the decomposition of DMP are further broken down to small acidic fragments of low solubility being released to gas phase, leaving the pH value of liquid essentially not altered for t longer than 60 min. The negligible effect of Nr on pH value as Nr is sufficiently high as 300 rpm or higher might be attributed to the balance of enhancement of gas liquid mass transfer and the purge of small acidic fragments by rotation stirring.

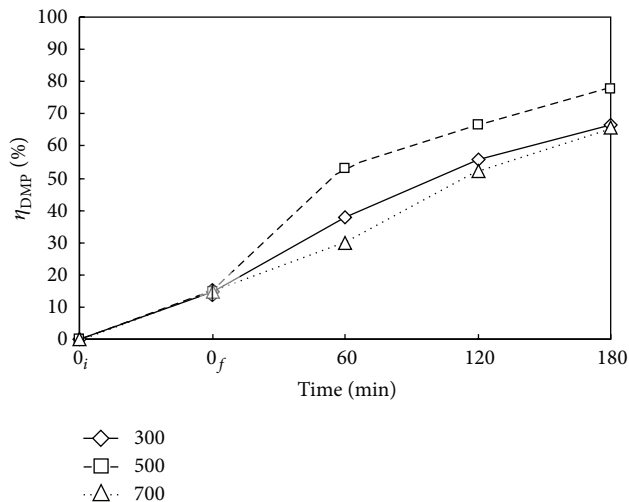


FIGURE 2: Time variation of decomposition efficiency of DMP (η_{DMP}) via WOP at various rotating speeds Nr. \diamond , \square , and \triangle : Nr = 300, 500, and 700 rpm. $C_0 = 100 \text{ mg L}^{-1}$, $V_L = 400 \text{ mL}$, $T = 473 \text{ K}$, and $P_T = 2.41 \text{ MPa}$. Working gas after time = 0_f is O_2 . \updownarrow : Mean and Standard deviation (SD, $n - 1$ method) at $t = 0_f$: 14.8 ± 2.8 .

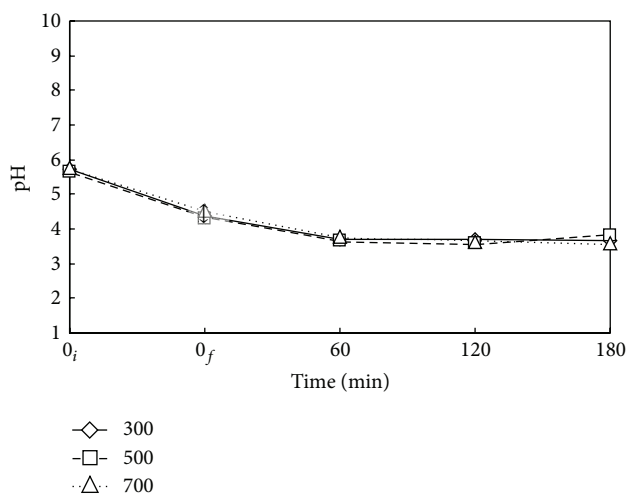


FIGURE 3: Time variation of pH value for the decomposition of DMP via WOP at various Nr. \diamond , \square , and \triangle : Nr = 300, 500, and 700 rpm. $C_0 = 100 \text{ mg L}^{-1}$, $V_L = 400 \text{ mL}$, $T = 473 \text{ K}$, and $P_T = 2.41 \text{ MPa}$. Working gas after time = 0_f is O_2 . \updownarrow : Mean and Standard deviation (SD, $n - 1$ method) at $t = 0_f$: 4.4 ± 0.1 .

3.2. Effects of Reaction Temperature T . Figures 4 and 5 show the time variations of η_{DMP} and η_{TOC} at reaction temperatures T of 463, 473, and 483 K for the case with Nr = 500 rpm and $P_T = 2.41 \text{ MPa}$. In the heating period from 0_i to 0_f without oxidant, DMP underwent mainly the hydrothermal decomposition accompanied with slight mineralization. The η_{DMP} is 17% for 463 and 473 K while 45% for 483 K at the end of heating period with no oxygen. The decomposition of DMP is very vigorous at high temperature. But the η_{TOC} is lower than 10% for all three temperatures because of the oxidant lack. With the presence of oxygen, the η_{DMP} was greatly enhanced

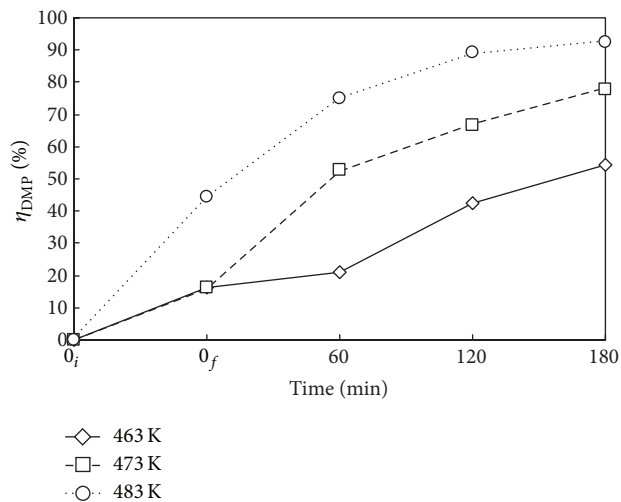


FIGURE 4: Time variation of η_{DMP} via WOP at various temperatures T . \diamond , \square , and \circ : $T = 463, 473,$ and 483 K . $C_0 = 100 \text{ mg L}^{-1}$, $V_L = 400 \text{ mL}$, $P_T = 2.41 \text{ MPa}$, and Nr = 500 rpm. Working gas after time = 0_f is O_2 .

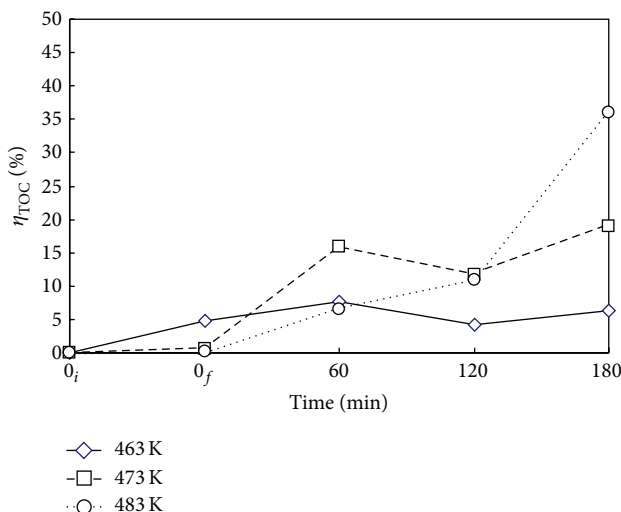


FIGURE 5: Time variation of mineralization efficiency of DMP (η_{TOC}) via WOP at various T . \diamond , \square , and \circ : $T = 463, 473,$ and 483 K . $C_0 = 100 \text{ mg L}^{-1}$, $V_L = 400 \text{ mL}$, $P_T = 2.41 \text{ MPa}$, and Nr = 500 rpm. Working gas after time = 0_f is O_2 .

while η_{TOC} moderately improved. The results indicated the low reactivity of acidic product fragments with oxygen. As expected, both η_{DMP} and η_{TOC} increased as reaction time and temperature increased. At $T = 483 \text{ K}$ and $t = 180 \text{ min}$, the η_{DMP} and η_{TOC} were 93 and 36%, respectively.

Figure 6 demonstrates the variation of pH value with time at various temperatures. As in Figure 3, the pH value decreased with time, while it levels off at a longer time depending on the temperature, for example, at 60 min for higher temperatures of 473 and 483 K while at 120 min for lower temperature of 464 K. Thus, a higher temperature case promotes the decomposition reaction, generally lowering and

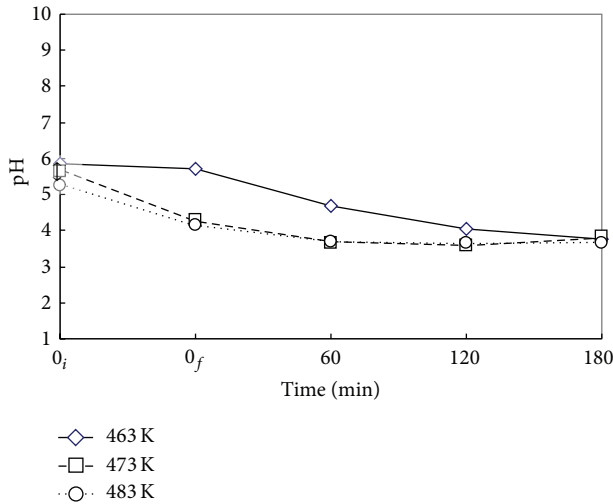


FIGURE 6: Time variation of pH value for the decomposition of DMP via WOP at various T . ◇, □, and ○: $T = 463, 473,$ and 483 K. $C_0 = 100 \text{ mg L}^{-1}$, $V_L = 400 \text{ mL}$, $P_T = 2.41 \text{ MPa}$, and $Nr = 500 \text{ rpm}$. Working gas after time = 0_f is O_2 . †: Mean and Standard deviation (SD, $n - 1$ method) at $t = 0_i$: 5.6 ± 0.3 .

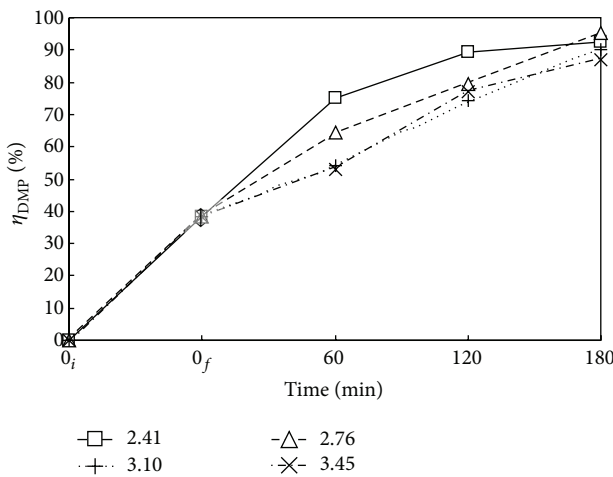


FIGURE 7: Time variation of η_{DMP} via WOP at various pressures. □, △, +, and ×: $P_T = 2.41, 2.76, 3.10,$ and 3.45 MPa . $C_0 = 100 \text{ mg L}^{-1}$, $V_L = 400 \text{ mL}$, $T = 483 \text{ K}$, and $Nr = 500 \text{ rpm}$. Working gas after time = 0_f is O_2 . †: Mean and Standard deviation (SD, $n - 1$ method) at $t = 0_f$: 38.2 ± 5.3 .

leveling the pH value faster than the lower temperature case. For 483 K, the pH value decreases to a leveling value of around 4 after 60 min.

3.3. Effects of Operation Pressure P_T . Figures 7 and 8 present the η_{DMP} and η_{TOC} versus time at P_T of 2.41, 2.76, 3.10, and 3.45 MPa with $Nr = 500 \text{ rpm}$ and $T = 483 \text{ K}$. Both η_{DMP} and η_{TOC} increase with time as expected. The oxygen was filled to reach the desired pressure right after heating period, that is, at $t = 0_f$. There is no oxidant in the time period from 0_i to 0_f . The DMP is hydrothermally decomposed in heating

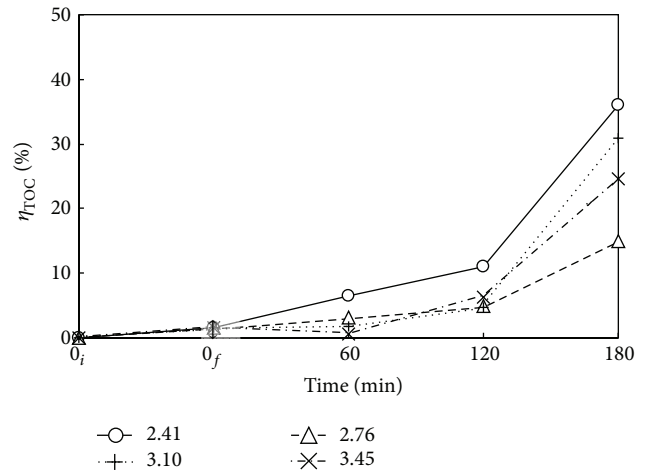


FIGURE 8: Time variation of η_{TOC} via WOP at various pressures. ○, △, +, and ×: $P_T = 2.41, 2.76, 3.10,$ and 3.45 MPa . $C_0 = 100 \text{ mg L}^{-1}$, $V_L = 400 \text{ mL}$, $T = 483 \text{ K}$, and $Nr = 500 \text{ rpm}$. Working gas after time = 0_f is O_2 . †: Mean and Standard deviation (SD, $n - 1$ method) at $t = 0_f$: 1.5 ± 1.3 .

period, giving η_{DMP} of around 33 to 45%. The DMP is only slightly mineralized with low η_{TOC} of about 0.3 to 3.1%. In the presence of oxygen, both η_{DMP} and η_{TOC} are enhanced as decomposition and mineralization proceed. The oxidative decomposition of DMP essentially consists of two-stage reversible reactions as illustrated in Figure 10, which is discussed in the next section. The decomposition of DMP and intermediates to short-chain aliphatic acid and then CO_2 are proposed by referring to the mechanism for the ozonation of DMP with UV and catalyst presented by Chang et al. [11]. An increase of oxygen as well as temperature enhances the forward reactions toward mineralization way, while the accumulation of CO_2 reversely inhibits the mineralization according to Le Chatelier's principle [31]. Thus, sufficient oxygen with satisfactorily high P_T is needed to ensure the forward oxidative decomposition reaction of DMP. For example, P_T at 2.41 MPa yields η_{DMP} and η_{TOC} of 93 and 36% at 180 min, respectively. Although higher P_T with more oxygen favors the forward decomposition reaction of DMP by oxygen, the absorption of accumulated gaseous products such as CO_2 and decomposed short-chain hydrocarbon fragments in the closed reaction system increases as P_T increases. The reabsorption of gaseous products back into the solution thus inhibits the forward reaction. Hence, as indicated in Figures 7 and 8, P_T of 2.41 MPa is more appropriate than those of 2.76 to 3.45 MPa.

Figure 9 plots pH value versus time at various P_T . The reduction of pH value in hydrothermal decomposition period is more vigorous than that in the oxidative decomposition period. The trend is similar to that of Figure 3 previously discussed. The increase of P_T higher than 2.41 MPa exhibits negligible effect on the pH value. The pH value levels off, indicating the limited oxidative mineralization to CO_2 and the gas liquid absorption balance of acidic compounds of CO_2 and decomposed short-chain hydrocarbon fragments.

TABLE 2: Comparison with some results of others for the decomposition of DMP via various methods.

Study	Method	Result
Bauer et al. [1]	Anaerobic process in field municipal landfill leachates	DMP was completely hydrolysis to phthalic acid but no cleavage for aromatic ring at different pH values
Wang et al. [16]	Electro-Fenton methods by electrodes: traditional graphite cathode (G), carbon nanotube sponge (CNTS), and graphite gas diffusion electrode (GDE)	η_{TOC} : G, 15%; GDE, 35%; CNTS, 75%
Souza et al. [17]	Electrochemical oxidation on F-doped Ti/ β -PbO ₂ anode in filter press reactor	DMP was completely decomposed under electrolyte Na ₂ SO ₄ and low current densities (10 mA), $\eta_{\text{TOC}} = 25\%$
Chang et al. [11]	Catalytic ozonation (OZ) in high-gravity rotating packed bed (HG) with catalyst (Pt/ Al_2O_3) and ultraviolet (UV) (mix of UV-C, UV-B, and UV-A with 200–280, 280–315, and 315–400 nm and with intensities of 3.73, 1.59, and 3.99 W m ⁻²)	η_{DMP} at 50 min: near 100% for Pt-OZ and UV-Pt-OZ η_{TOC} at 1 h: 45% (OZ); 56% (UV-OZ); 57% (Pt-OZ); 68% (UV-Pt-OZ)
Chen et al. [13]	Photocatalytic degradation using magnetic poly(methyl methacrylate) (mPMMA) and UV 254 nm	η_{DMP} at 4 h: 55–100% via TiO ₂ /mPMMA (C1); 68–100% via Pt-TiO ₂ /mPMMA (C2) η_{TOC} at 4 h: 7.5–37.5 % via C1; 11–64% via C2
Chen et al. [19]	Photocatalytic ozonation using TiO ₂ , Al ₂ O ₃ , and TiO ₂ /Al ₂ O ₃ catalysts	η_{DMP} at 30 min: 2–22% without O ₃ , 90–100% with O ₃ . η_{TOC} : 16–93%, 32–97% at 1, 4 h
Chen et al. [12]	Photocatalysis using magnetic Pt-TiO ₂ /mPMMA	UV 185 nm contributes better removal efficiency than UV 254 nm
This study	Wet oxygen oxidation	η_{DMP} and η_{TOC} are 93 and 36% at Nr = 500 rpm, T = 483 K, P _T = 2.41 MPa, and t = 180 min

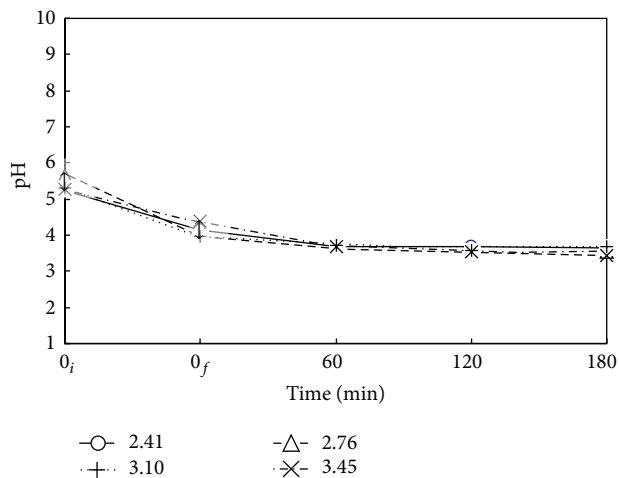


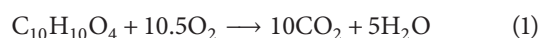
FIGURE 9: Time variation of pH value for decomposition of DMP via WOP at various pressures. \circ , \triangle , $+$, and \times : $P_T = 2.41, 2.76, 3.10$, and 3.45 MPa. $C_0 = 100 \text{ mg L}^{-1}$, $V_L = 400 \text{ mL}$, $T = 483 \text{ K}$, and $\text{Nr} = 500 \text{ rpm}$. Working gas after time = 0_f is O₂. \updownarrow : Mean and Standard deviation (SD, $n - 1$ method) at $t = 0_i$: 5.2 ± 0.2 and at $t = 0_f$: 4.1 ± 0.2 .

It is noted that the P_T was the sum of partial pressures of oxygen (P_{O_2}) and water vapor (P_{WV}). The saturation P_{WV} varies with temperature and is about 2.3 MPa at 483 K [27]. Setting P_T at 2.41 and 3.45 MPa gave P_{O_2} of 0.11 and 1.15 MPa, respectively, for supplying the oxygen for mineralization reaction. Referring to the study of Lin and Ho [27] using

2.5 MPa as the lowest setting at 473 K, this analysis thus did not employ P_T lower than 2.41 MPa at 483 K.

3.4. Mechanism of Two-Stage Decomposition of DMP via WOP. In this test, the reactions are involved in components of DMP, oxygen, intermediate products, and ultimate end products of CO₂ and H₂O. The intermediates are the decomposed short-chain hydrocarbon fragments which are acidic as reflected by the low pH value. Accordingly, the mechanism of two-stage decomposition of DMP via WOP may be depicted in Figure 10. In the heating stage without oxygen, DMP is essentially hydrothermally decomposed to acidic fragments lowering the pH value with significant η_{DMP} , while forming little CO₂ with low η_{TOC} . With the introduction of oxygen in the second stage, oxidation of DMP and its decomposed fragments takes place, destructing them into short-chain acids such as aliphatic acids or more completely to CO₂ and H₂O. The produced CO₂, however, was kept within the closed-batch reaction system in this study.

The stoichiometry equation for the forward oxidation reaction of DMP can expressed as follows:



For complete mineralization of DMP, each mole DMP consumes 10.5 moles of O₂ while producing 10 moles of CO₂. The CO₂ partial pressure contributed from the complete mineralization of DMP is about 0.045 MPa by consuming 0.047 MPa O₂. This reaction reduces the total pressure slightly. In fact, the oxygen is not a limited factor because

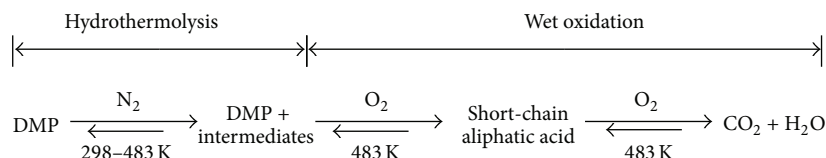


FIGURE 10: Two stages for the decomposition of DMP via WOP.

the minimum pressure applied is 2.41 MPa exceeding the need. However, the mineralization of reaction (1) is hindered by the accumulation of product CO_2 in the closed-batch reaction system. It forces the backward reaction of reaction (1) according to Le Chatelier's principle [31]. The equilibrium balance of the forward and backward reaction thus limits the complete mineralization of DMP. A release of CO_2 gas out from the reaction system would certainly assist approaching the complete mineralization of DMP.

3.5. Comparison with Results of Others. Comparison of the results of this study with others is illustrated in Table 2. The present WOP can reach η_{DMP} of 93% as high as the advanced methods (AMs) of electrochemical oxidation, photocatalytic degradation, and photocatalytic ozonation. The η_{TOC} of WOP of 36% is lower than those of the aforementioned AMs at some conditions, however, comparable at other conditions. It is noted that the WOP simply uses oxygen with demand of the thermal energy, while other AMs need to employ chemical agents, catalysts, and ozone along with electric or UV energies. Thus, the WOP is comparatively simple to apply. The discrepancy of incomplete mineralization of WOP may be consummated with the postbiological treatment if necessary [20]. The predecomposition of DMP by WOP certainly greatly enhances the followed biological processing.

4. Conclusions

This study treated the toxic endocrine disrupter substance (EDC) of DMP via wet oxidation using oxygen (WOP) without other oxidant additives, being beneficial to the subsequent biological process if necessary, while avoiding the treatment of unwanted oxidant residues. The WOP effectively decomposed the DMP, indicating its feasible application for the treatment of other EDCs.

Among the three factors investigated, namely, rotation speed N_r , reaction temperature T , and operation pressure P_T , the effects of T are most significant. The proper conditions found are at 483 K, 2.41 MPa, and 500 rpm. The η_{DMP} and η_{TOC} of 93% and 36%, respectively, can be achieved at 180 min. The produced CO_2 kept in the closed-batch reaction system seems to resist the further mineralization reaction from intermediates. The application of sequential release of CO_2 while addition of O_2 to improve the η_{TOC} is thus suggested.

Conflict of Interests

The authors declare that there is no conflict of interests regarding the publication of this paper.

Acknowledgment

The authors are grateful for the financial supports of this research provided by the Ministry of Science and Technology (formerly the National Science Council) of Taiwan.

References

- [1] M. J. Bauer, R. Herrmann, A. Martin, and H. Zellmann, "Chemodynamics, transport behaviour and treatment of phthalic acid esters in municipal landfill leachates," *Water Science and Technology*, vol. 38, no. 2, pp. 185–192, 1998.
- [2] M. Zhang, S. Liu, H. Zhuang, and Y. Hu, "Determination of dimethyl phthalate in environment water samples by a highly sensitive indirect competitive ELISA," *Applied Biochemistry and Biotechnology*, vol. 166, no. 2, pp. 436–445, 2012.
- [3] J. P. Sumpter, "Endocrine disrupters in the aquatic environment: an overview," *Acta Hydrochimica et Hydrobiologica*, vol. 33, no. 1, pp. 9–16, 2005.
- [4] C. A. Staples, D. R. Peterson, T. F. Parkerton, and W. J. Adams, "The environmental fate of phthalate esters: a literature review," *Chemosphere*, vol. 35, no. 4, pp. 667–749, 1997.
- [5] W. Den, H. C. Liu, S. F. Chan, K. T. Kin, and C. Huang, "Adsorption of phthalate esters with multiwalled carbon nanotubes and its application," *Journal of Environmental Engineering and Management*, vol. 16, no. 4, pp. 275–282, 2006.
- [6] A. J. Kumar and C. Namasivayam, "Uptake of endocrine disruptor bisphenol-A onto sulphuric acid activated carbon developed from biomass: equilibrium and kinetic studies," *Sustainable Environment Research*, vol. 24, no. 1, pp. 73–80, 2014.
- [7] M. F. N. Secondes, V. Naddeo, F. J. Ballesteros, and V. Belgiorno, "Adsorption of emerging contaminants enhanced by ultrasound irradiation," *Sustainable Environment Research*, vol. 24, no. 5, pp. 349–355, 2014.
- [8] D. W. Liang, T. Zhang, H. H. P. Fang, and J. He, "Phthalates biodegradation in the environment," *Applied Microbiology and Biotechnology*, vol. 80, no. 2, pp. 183–198, 2008.
- [9] D. L. Wu, B. L. Hu, P. Zheng, and Q. Mahmood, "Anoxic biodegradation of dimethyl phthalate (DMP) by activated sludge cultures under nitrate-reducing conditions," *Journal of Environmental Sciences*, vol. 19, no. 10, pp. 1252–1256, 2007.
- [10] D. L. Wu, Q. Mahmood, L. L. Wu, and P. Zheng, "Activated sludge-mediated biodegradation of dimethyl phthalate under fermentative conditions," *Journal of Environmental Sciences*, vol. 20, no. 8, pp. 922–926, 2008.
- [11] C.-C. Chang, C.-Y. Chiu, C.-Y. Chang et al., "Combined photolysis and catalytic ozonation of dimethyl phthalate in a high-gravity rotating packed bed," *Journal of Hazardous Materials*, vol. 161, no. 1, pp. 287–293, 2009.

- [12] Y.-H. Chen, L.-L. Chen, and N.-C. Shang, "Photocatalytic degradation of dimethyl phthalate in an aqueous solution with Pt-doped TiO₂-coated magnetic PMMA microspheres," *Journal of Hazardous Materials*, vol. 172, no. 1, pp. 20–29, 2009.
- [13] Y.-H. Chen, N.-C. Shang, L.-L. Chen et al., "Photodecomposition of dimethyl phthalate in an aqueous solution with UV radiation using novel catalysts," *Desalination and Water Treatment*, vol. 52, no. 16–18, pp. 3377–3383, 2014.
- [14] Y. Jing, L. Li, Q. Zhang, P. Lu, P. Liu, and X. Lü, "Photocatalytic ozonation of dimethyl phthalate with TiO₂ prepared by a hydrothermal method," *Journal of Hazardous Materials*, vol. 189, no. 1–2, pp. 40–47, 2011.
- [15] W. Jiang, J. A. Joens, D. D. Dionysiou, and K. E. O'Shea, "Optimization of photocatalytic performance of TiO₂ coated glass microspheres using response surface methodology and the application for degradation of dimethyl phthalate," *Journal of Photochemistry and Photobiology A: Chemistry*, vol. 262, pp. 7–13, 2013.
- [16] Y. Wang, Y. Liu, T. Liu et al., "Dimethyl phthalate degradation at novel and efficient electro-Fenton cathode," *Applied Catalysis B: Environmental*, vol. 156–157, pp. 1–7, 2014.
- [17] F. L. Souza, J. M. Aquino, K. Irikura, D. W. Miwa, M. A. Rodrigo, and A. J. Motheo, "Electrochemical degradation of the dimethyl phthalate ester on a fluoride-doped Ti/β-PbO₂ anode," *Chemosphere*, vol. 109, pp. 187–194, 2014.
- [18] F. Charest and E. Chornet, "Wet oxidation of active carbon," *Canadian Journal of Chemical Engineering*, vol. 54, no. 6, pp. 190–196, 1976.
- [19] Y.-H. Chen, D.-C. Hsieh, and N.-C. Shang, "Efficient mineralization of dimethyl phthalate by catalytic ozonation using TiO₂/Al₂O₃ catalyst," *Journal of Hazardous Materials*, vol. 192, no. 3, pp. 1017–1025, 2011.
- [20] M. J. Dietrich, T. L. Randall, and P. J. Canney, "Wet air oxidation of hazardous organics in wastewater," *Environmental Progress*, vol. 4, no. 3, pp. 171–177, 1985.
- [21] S. Imamura, H. Kinunaka, and N. Kawabata, "The wet oxidation of organic compounds catalyzed by Co-Bi complex oxide," *Bulletin of the Chemical Society of Japan*, vol. 55, no. 11, pp. 3679–3680, 1982.
- [22] M. M. Ito, K. Akita, and H. Inoue, "Wet oxidation of oxygen- and nitrogen-containing organic compounds catalyzed by cobalt(III) oxide," *Industrial & Engineering Chemistry Research*, vol. 28, no. 7, pp. 894–899, 1989.
- [23] J. Levec, M. Herskowitz, and J. M. Smith, "Active catalyst for oxidation of acetic-acid solutions," *AIChE Journal*, vol. 22, no. 5, pp. 919–920, 1976.
- [24] L. X. Li, P. S. Chen, and E. F. Gloyna, "Generalized kinetic-model for wet oxidation of organic-compounds," *AIChE Journal*, vol. 37, no. 11, pp. 1687–1697, 1991.
- [25] W. H. Li, J. L. Huang, H. Wang, A. J. Qi, and J. Xie, "Treatment of acrylic acid waste water by catalytic wet oxidation," *Journal of Jilin Institute of Chemical Technology*, vol. 24, no. 3, pp. 3–6, 2007.
- [26] S. H. Lin and Y. F. Wu, "Catalytic wet air oxidation of phenolic wastewaters," *Environmental Technology*, vol. 17, no. 2, pp. 175–181, 1996.
- [27] S. H. Lin and S. J. Ho, "Treatment of high-strength industrial wastewater by wet air oxidation—a case study," *Waste Management*, vol. 17, no. 1, pp. 71–78, 1997.
- [28] H. Lin Sheng and S. J. Ho, "Kinetics of wet air oxidation of high-strength industrial wastewater," *Journal of Environmental Engineering*, vol. 123, no. 9, pp. 852–858, 1997.
- [29] V. S. Mishra, V. V. Mahajani, and J. B. Joshi, "Wet air oxidation," *Industrial and Engineering Chemistry Research*, vol. 34, no. 1, pp. 2–48, 1995.
- [30] A. Sadana and J. R. Katzer, "Catalytic oxidation of phenol in aqueous solution over copper oxide," *Industrial and Engineering Chemistry*, vol. 13, no. 2, pp. 127–134, 1974.
- [31] P. W. Atkins, "Principles of chemical equilibrium," in *The Elements of Physical Chemistry*, chapter 7, Oxford University Press, Oxford, UK, 3rd edition, 1993.



Hindawi

Submit your manuscripts at
<http://www.hindawi.com>

